Composite Films of Poly(vinyl alcohol) and Bifunctional Cross-linking Cellulose Nanocrystals

Juho Antti Sirviö,[*,†] Samuli Honkaniemi,[†] Miikka Visanko,[‡] and Henrikki Liimatainen[†]

[†]Fibre and Particle Engineering, University of Oulu, P.O. Box 4300, FI-90014 Oulu, Finland
[‡]Fibre and Particle Engineering and Thule Institute, University of Oulu, P.O. Box 4300, FI-90014 Oulu, Finland

ABSTRACT: Long and flexible cellulose nanofibrils or stiff and short cellulose nanocrystals (CNCs) are both promising lightweight materials with high strength and the potential to serve as reinforcing agents in many polymeric materials. In this study, bifunctional reactive cellulose nanocrystals (RCNCs) with carboxyl and aldehyde functionalities were used as reinforcements to prepare acetal-bonding cross-linked poly(vinyl alcohol) (PVA) films. Two RCNCs were obtained through the mechanical homogenization of partially carboxylated dialdehyde cellulose (DAC) with a residual aldehyde content of 0.55 and 1.93 mmol/g and a carboxyl content of 1.65 and 1.93 mmol/g, respectively. The mechanical, thermal, and barrier properties of PVA-RCNC films with a variable mass ratio of RCNCs (0.5−10%) were determined. Reference CNCs without reactive aldehydes were obtained through the reduction of aldehyde functionalities to primary hydroxide groups, and their reinforcing effect was compared to RCNCs. With the addition of 10% acetal-bonding RCNCs with respect to PVA weight, the tensile strength and Young's modulus were up to 2-fold greater than those of pure PVA film. An addition of only 0.5% RCNCs improved the tensile strength of the PVA film by 66% and the modulus by 61%. In comparison, a significantly lower reinforcing effect (19% with CNC loading of 0.5%) was found using reference CNCs. PVA's effective oxygen barrier and thermal properties were preserved when RCNCs were introduced into the films.

KEYWORDS: regioselective oxidation, nanocellulose, poly(vinyl alcohol) film, cross-linking, barrier, mechanical properties
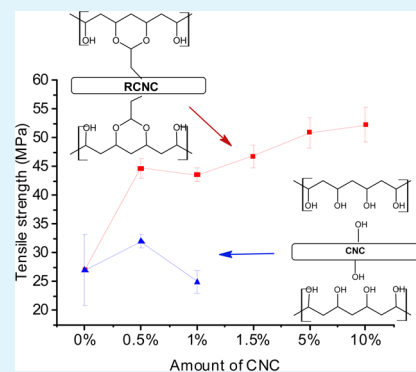
INTRODUCTION

Nanocellulose has attracted a great deal of interest in scientific and industrial research due to its advanced properties compared to traditional cellulosic fibers and oil-based materials. Some of the well-known characteristics of nanocellulose are that it has high mechanical strength,[1] is lightweight,[2] and has a greater specific surface area,[3] all of which make it more valuable than its macro-scale counterparts. The fact that nanocellulose is obtained from one of the most abundant and widely available renewable polymers, cellulose, makes it a sustainable and economically attractive raw material. Moreover, nanocellulose is generally recognized as having low toxicity, although different toxicity profiles[4,5] exist.

There are several techniques to produce nanocellulose. For plant-derived cellulose such as wood fibers, the primary production methods are based on the pure mechanical disintegration of cellulose fibers or a combination of chemical pretreatment and mechanical comminution to obtain nanofibrillated cellulose (NFC).[6] The stiff, rod-like particles known as cellulose nanocrystals (CNCs)[7] are commonly produced using strong acid hydrolysis in which the amorphous regions of cellulose are dissolved.[7] CNCs can also be produced through acid-free methods using ultrasonic-assisted (2,2,6,6-tetramethylpiperidin-1-yl)oxyl (TEMPO) oxidation,[8] ammonium persulfate oxidation,[9] and sequential oxidation and reductive amination.[10]

Nanocellulosic components that are strong and lightweight can function as potential reinforcing agents in various synthetic[11−13] and natural polymers.[14−16] Of the synthetic polymers, biodegradable poly(vinyl alcohol) (PVA) is widely studied, and it is considered to be a more environmentally feasible alternative to polymers such as polyethylene.[17] PVA also has good thermal stability, optical properties, and high oxygen barrier properties, and it has been used in many applications, including filters,[18] packaging,[19] and tissue engineering scaffolds.[20] PVA is also recognized as a suitable candidate for incorporation into multilayer coatings of organic solar cells.[21] To expand the feasibility of PVA in applications requiring high mechanical strength and stiffness, nanocellulose has been studied as a reinforcing agent for PVA films,[22,23] fibers,[24,25] and hydrogels.[26] One drawback, however, has been the agglomeration of nanocellulosic reinforcement, especially at higher cellulose loads, leading to a decrease in the reinforcement effect.[27]

For the proper reinforcing effect, a good interaction between the matrix and the nanocellulosic fillers is a prerequisite. Several different modifications such as hydrophobization[28] or cross-linking with the matrix[14,29,30] have been used to improve the reinforcing effect of nanocellulose. In the present study, novel

bifunctional reactive cellulose nanocrystals (RCNCs) with carboxyl and aldehyde functionalities were produced using sequential periodate and partial chlorite oxidations of wood cellulose fibers. Due to the ability of aldehydes to form stable cyclic acetal bonds with hydroxyl groups of PVA, RCNCs were studied as cross-linking reinforcing agents for PVA. Chemical modifications were conducted in aqueous media prior to the liberation of CNCs through mechanical disintegration, thus excluding the energy-demanding and time-consuming purification of CNCs. The morphology of RCNCs was analyzed using a transmission electron microscope (TEM) and UV−visible spectroscopy, and the tensile, barrier, and thermal properties of solvent-cast RCNC-PVA films were studied. Crystallinity and surfaces of PVA films were studied using wide-angle X-ray diffraction (WAXD) and field emission scanning electron microscopy (FESEM), respectively. The chemical modifications of cellulose were characterized using diffuse reflectance infrared Fourier transform (DRIFT). CNCs with no residual aldehyde functionalities were used as the reference reinforcing agents.

■ MATERIALS AND METHODS

Materials. Bleached birch pulp (*Betula pendula*) was obtained as dry sheets and used as a cellulose source of RCNCs after disintegration in deionized water. The properties of the cellulose fibers are presented elsewhere.[31] The p.a. grade chemicals used for the periodate and chlorite oxidations ($NaIO_4$, $NaClO_2$ [purity of 80%]), the borohydride reduction ($NaBH_4$, $NaH_2PO_4 \cdot H_2O$), and the aldehyde and carboxyl content analyses ($NH_2OH \cdot HCl$, $CH_3COONa \cdot 2H_2O$, NaCl, and NaOH) were obtained from Sigma-Aldrich (Germany) and were used without further purification. PVA (Mowiol 3-96, 96.8−97.6 mol % hydrolysis) was obtained from Sigma-Aldrich (Germany). Deionized water was used throughout the experiments.

Preparation of Reactive Cellulose Nanocrystals. A two-step reaction was used to prepare bifunctional RCNCs with carboxyl and aldehyde functionalities. First, the reactive aldehyde groups were introduced to cellulose using periodate oxidation, after which the aldehydes were partially converted to carboxyl groups using chlorite oxidation. Pulp samples were first oxidized with sodium metaperiodate by weighing 12 g abs of cellulose into a 2000 mL flask and adding 1200 mL of deionized water and 9.84 g of $NaIO_4$ to produce dialdehyde celluloses, dialdehyde cellulose (DAC) 1 and 2. Water baths at 65 and 75 °C were used for the DAC 1 and 2, respectively, and LiCl (21.6 g) was used as a metallic salt activator in the suspension of DAC 2. The reaction vessels were covered with aluminum foil to prevent the photoinduced decomposition of periodate. After 3 h, the products were filtered and washed several times with deionized water to remove iodine-containing compounds. The aldehyde content of the oxidized cellulose was determined by an oxime reaction as reported previously.[32]

Aldehyde groups of DACs were then partially oxidized to carboxylic acid groups using sodium chlorite in a manner similar to that reported previously.[33] At first, 2 g abs of DAC was dispersed in 44.4 mL of deionized water by mixing for 1 min at 11 000 rpm with an Ultra-Turrax mixer (IKA T25, Germany) followed by the addition of sodium chlorite (1.24 g for DAC1 and 2.18 g for DAC2) dissolved in 12% acetic acid. The reaction proceeded for 8 min, after which the dispersion was filtered and washed with 2000 mL of water, redispersed in 2000 mL of water, filtered, and finally washed with 2000 mL of water. The product was stored at 4 °C in a nondried state. Partially oxidized DAC1 and DAC2 were designated as PO-DAC1 and PO-DAC2, respectively.

RCNCs were produced from PO-DAC1 and PO-DAC2 through mechanical disintegration by using a microfluidizer (Microfluidics M-110EH-30). Before disintegration, the pH of both PO-DAC dispersions was adjusted to 7 by using a dilute NaOH solution. Dispersions were then diluted to a 0.5% concentration and disintegrated with one pass through 400 and 200 μm chambers at a

pressure of 1300 bar, then passed once through 400 and 100 μm chambers at a pressure of 2000 bar, and last, passed once through 200 and 87 μm chambers at a pressure of 2000 bar. Reactive CNCs obtained from PO-DAC1 and PO-DAC2 were designated as RCNC1 and RCNC2, respectively. The carboxylic acid content of chlorite-oxidized DAC was determined via conductometric titration using a procedure described in the literature.[34,35]

The reference CNC was prepared from PO-DAC1 through the reduction of residual aldehydes using sodium borohydride in manner similar to that described in the literature.[36] First, 2 g abs of PO-DAC1 was mixed with 500 mL of deionized water, and then, 0.69 g of sodium dihydrogen phosphate monohydrate was added, followed by the addition of 1 g of sodium borohydride. The reaction proceeded under mixing for 4 h, followed by the removal of the chemicals using filtration. The product was washed with 2000 mL of water, redispersed in 2000 mL of water, filtered, washed again with 2000 mL of water, and stored at 4 °C in a nondried state. The partially oxidized and reduced DAC sample was designated as PO-PR-DAC. PO-PR-DAC was disintegrated into CNCs using the same procedure used to obtain RCNCs and was then designated as CNC-ref.

Preparation of RCNC-Reinforced PVA Films. Films were prepared using a solvent-casting method. First, 1.515 g of PVA was dissolved in 150 mL of deionized water at 90 °C in a round-bottom flask. The flask was then transferred to a 40 °C water bath, after which the desired amount of RCNCs (0.5−10% with respect to PVA content) and a 0.1 M HCl solution (30% mol compared to the residual aldehyde content) was added. After mixing for 4 h, the solution was degassed under vacuum suction and cast in a polystyrene tray measuring 505 cm^2, resulting in films with a grammage of 30 g/m^2. After drying for about 5 days, the films were conditioned at 50% relative humidity (RH) for 1 day and carefully peeled off from the molds. Reference films of PVA without the addition of CNCs and HCl and a film containing CNC-ref were produced in a similar manner as the RCNC-reinforced films.

Mechanical Properties. The tensile tests were performed with a universal material testing machine (Instron 5544, USA) equipped with a 100 N load cell. The PVA-RCNC films were cut into thin strips with a specimen width of 5 mm. For the tensile testing, a 40 mm gauge length was set under a strain rate of 4 mm/min and six specimens were measured. Using a Lorentzen & Wettre thickness tester (Sweden), the thickness of each specimen was determined as an average from five random locations on the specimen. Film thicknesses ranged from 14 to 44 μm. The tests were conducted in 50% RH at a temperature of 23 °C and under a prestrain of 0.05−0.1 N. The specimens were conditioned for 1 day in the measurement environment before testing. The Young's modulus was calculated from the initial linear portion of the stress−strain curve, and the ultimate tensile strength was defined as the stress at the specimen breakage.

Transmission Electron Microscopy. The morphological features of the fabricated RCNCs were analyzed with a Tecnai G2 Spirit transmission electron microscope (FEI Europe, Eindhoven, The Netherlands). Samples were prepared by diluting each sample with Milli-Q water. A small droplet of the dilution was dosed on top of a Butvar-coated copper grid. Any excess amount of the sample was removed from the grid by touching the droplet with a corner of filter paper. Samples were negatively stained by placing a droplet of uranyl acetate (2% w/v) on top of each specimen. The excess amount of the uranyl acetate was removed with filter paper as described above. The grids were dried at room temperature and analyzed at 100 kV under standard conditions. Images were captured using a Quemesa CCD camera and the CNC's morphology in terms of width and length was measured using iTEM image analysis software (Olympus Soft Imaging Solutions GMBH, Munster, Germany). In total, 50 CNCs of each sample were measured. The final results were averaged, and standard deviations were calculated.

Optical Transmittance. The transmittance of 0.1% for the nanocellulose suspensions was measured at wavelengths of 300−800 nm using Shimadzu UV−visible spectroscopy (Japan).

Thermal Analyses. Thermogravimetric (TGA) analyses were conducted using a Netzsch STA 449 F3 apparatus. TGA conditions

Scheme 1. Synthesis of Bifunctional Cellulose with Aldehyde and Carboxylic Acid Groups (PO-DAC) and a Reduction of Residual Aldehydes with Borohydride (PO-PR-DAC)[a]
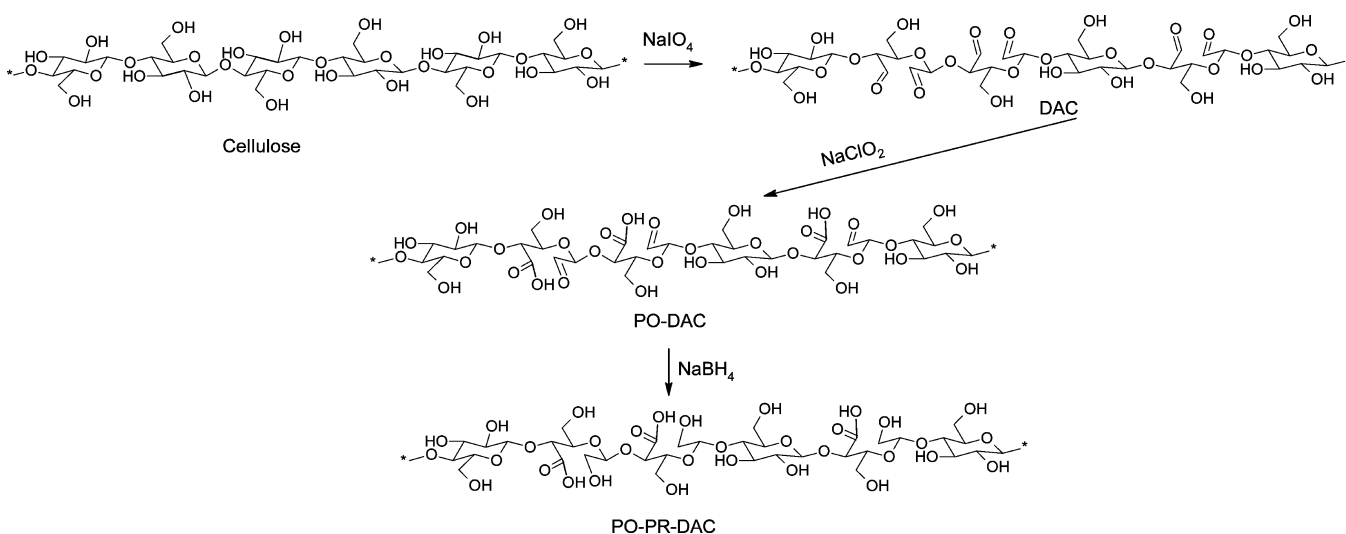
[a]The ratio of chemical groups is indicative.

included a nitrogen atmosphere with a flow rate of 30 mL/min, a heating rate of 10 °C/min, a temperature range of 25−600 °C, a sample mass between 5 and 7 mg, and aluminum pans.

Barrier against Oxygen and Water Vapor. The oxygen transmission rate (OTR) of the films was measured using a MOCON OxTran 2/20 (Minneapolis, MN). The film was exposed to 100% oxygen on one side and to oxygen-free nitrogen on the other side. The oxygen permeability (OP) was calculated by multiplying the OTR by the thickness of the film and dividing it by the difference in the partial pressure of the oxygen gas between the two sides of the film. The measurements were made at 23 °C, a normal atmospheric pressure, and a 50% RH with a specimen area of 5 cm². The OP was determined as duplicates.

The water vapor transmission rate (WVTR) of the films was measured using MOCON Permatran (Minneapolis, MN). The measurements were made at 37 °C, a normal atmospheric pressure, and a 50% RH with a specimen area of 5 cm². The WVTR was determined as duplicates.

Field Emission Scanning Electron Microscopy. FESEM images of the uncoated PVA films were obtained using Sigma HD VP FE-SEM (Zeiss, Germany). The accelerating voltage during imaging was 3 kV.

X-ray Diffraction. The crystallinity of the PVA films was analyzed using WAXD. Measurements were conducted on a Siemens D5000 diffractometer (Germany) equipped with a Cu Kα radiation source (λ = 0.1542 nm). Scans were taken over a 2θ (Bragg angle) range from 5° to 50° at a scanning speed of 0.1° s⁻¹ using a step time of 5 s. The degree of crystallinity in terms of the crystallinity index (CrI) was calculated according to the following eq 1:

$$CrI = \frac{A_C}{(A_C + A_a)} \times 100\%$$ (1)

where A_a is experimental integrated intensity of amorphous phase and A_c is experimental integrated intensity of crystalline phase.[37,38]

■ RESULTS AND DISCUSSION

Preparation of RCNCs. RCNCs were produced using sequential periodate and chlorite oxidation. The periodate oxidation of cellulose results in the formation of DAC, which was then partially oxidized with sodium chlorite. As a result, bifunctional cellulose with both carboxylic acid and aldehyde groups was produced. The aldehyde content of DAC1 and DAC2 after periodate oxidation was 2.20 and 3.86 mmol/g,
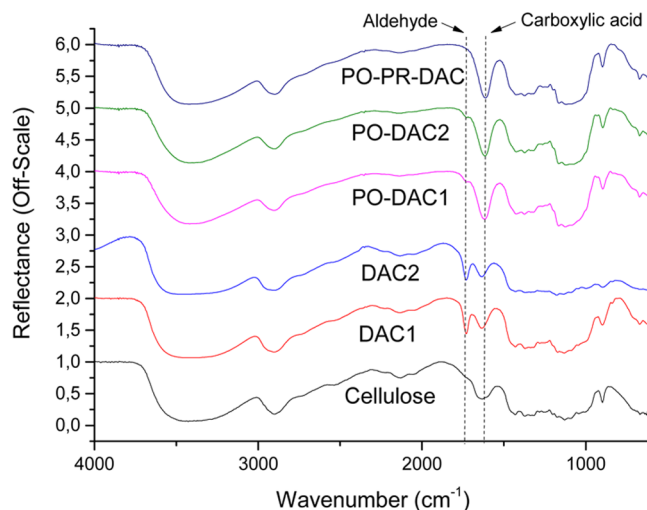

Figure 1. DRIFT spectra of original and chemically modified cellulose. The aldehyde and carboxylic acid bands at 1730 and 1615 cm⁻¹, respectively, are indicated by the dashed lines.

respectively, as determined by elemental analysis of the oxime derivate of DAC.[32] After partial chlorite oxidation, the carboxylic acid content of PO-DAC1 and PO-DAC2 was 1.65 and 1.93 mmol/g, respectively, as determined by conducto-metric titration. The residual aldehyde content after chlorite oxidation was 0.55 and 1.93 mmol/g for PO-DAC1 and PO-DAC2, respectively. As a reference, CNC without aldehyde functionalities was prepared as a sodium borohydride reduction of PO-DAC1. Sodium borohydride is known to reduce the aldehyde functionalities of DAC to corresponding hydroxyl groups.[36] Scheme 1 presents the PO-DAC and PO-PR-DAC syntheses.

DRIFT spectra confirmed the chemical modifications of cellulose (Figure 1). After periodate oxidation, a new band at 1730 cm⁻¹, corresponding to the C═O stretching of aldehyde, was observed. Significant reduction in the aldehyde band was noticed after partial chloride oxidation of DAC, along with the appearance of a new band at 1615 cm⁻¹. This band is attributed
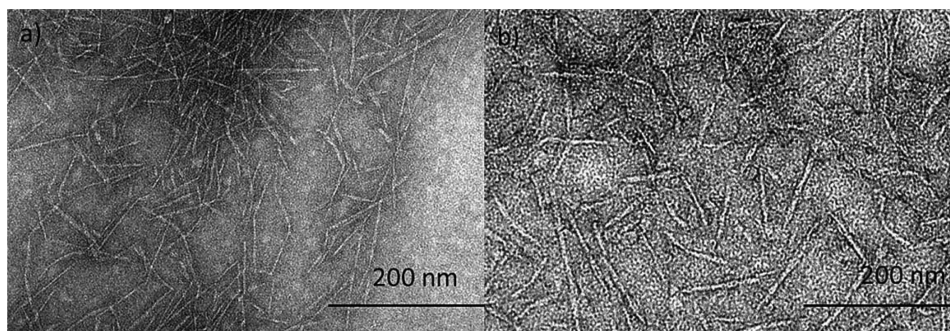
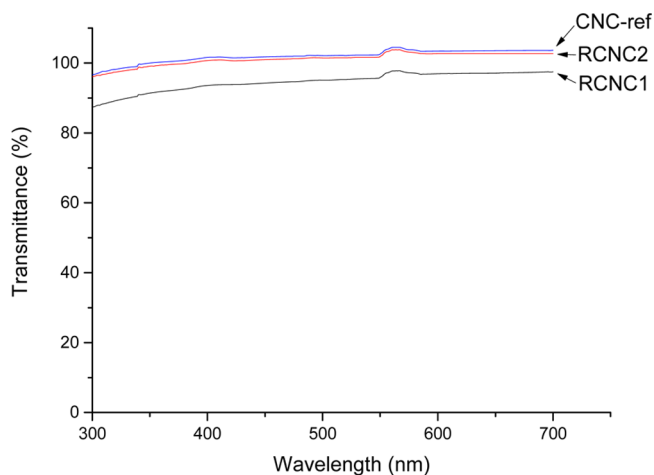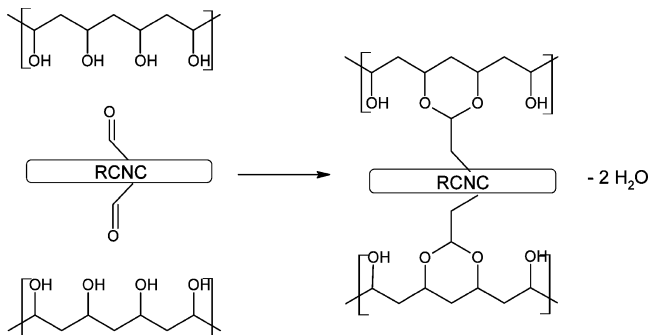**Figure 2.** TEM images of (a) RCNC1 and (b) RCNC2.

Figure 3. Optical transmittance of CNC suspensions (0.1% w/w).

Scheme 2. Schematic Illustration of the Acetal Crosslinking of PVA with the Aldehyde Groups of RCNCs

to C=O stretching of the deprotonated carboxylic group (spectra were recorded from PO-DACs at pH 7). The C=O band of the aldehyde disappeared after the borohydride reduction, indicating that residual aldehydes were converted to hydroxyl groups.

We have previously shown that periodate-oxidized cellulose can be converted to CNCs after sequential chemical modification and mechanical comminution without a strong acid treatment.[10] Short nanocrystals are formed by the erosion of cellulose fiber, leading to dissolution of amorphous regions and cutting of the fibers.[39] Here, both bifunctionalized cellulose samples (PO-DACs) were easily disintegrated into highly transparent, low-viscose solutions (RCNC 1 and 2) using a microfluidizer. TEM images confirmed the presence of individualized cellulose nanocrystals (Figure 2). The lateral dimensions of RCNC1 and RCNC2 were 2.82 ± 0.99 and 4.55 ± 1.20 nm, respectively, and the lengths of the individual nanocrystals were 84 ± 34 and 108 ± 40 nm for RCNC 1 and 2, respectively. Some web-like structures containing longer cellulose nanofibrils were observed in the case of RCNC1, but RCNC2 mainly consisted of CNCs without elongated nanofibrils. These results are consistent with our previous results obtained for amphiphilic CNCs.[10]

All of the CNC samples exhibited very high transmittance at the visible light range (300−400 nm), as shown in Figure 3. The transmittance of RCNC1 was 97% at a wavelength of 600 nm, whereas both RCNC2 and CNC1 had a transmittance of around 100%. The results confirm the efficient disintegration of cellulose fibers into uniformly occurring CNCs with only a small fraction of aggregated cellulose nanofibrils remaining. The transmittance results are significantly higher than in our previous study of reductive aminated DAC,[10] indicating a good disintegration efficiency of highly charged PO-DACs.

Composite Films of PVA and Bifunctional Cross-Linking CNCs. The hydroxyl groups of PVA can potentially

Figure 4. Appearance of PVA film and composite films with 0.5% of RCNC1, RCNC2, and CNC-ref and 10% of RCNC1 and RCNC2.
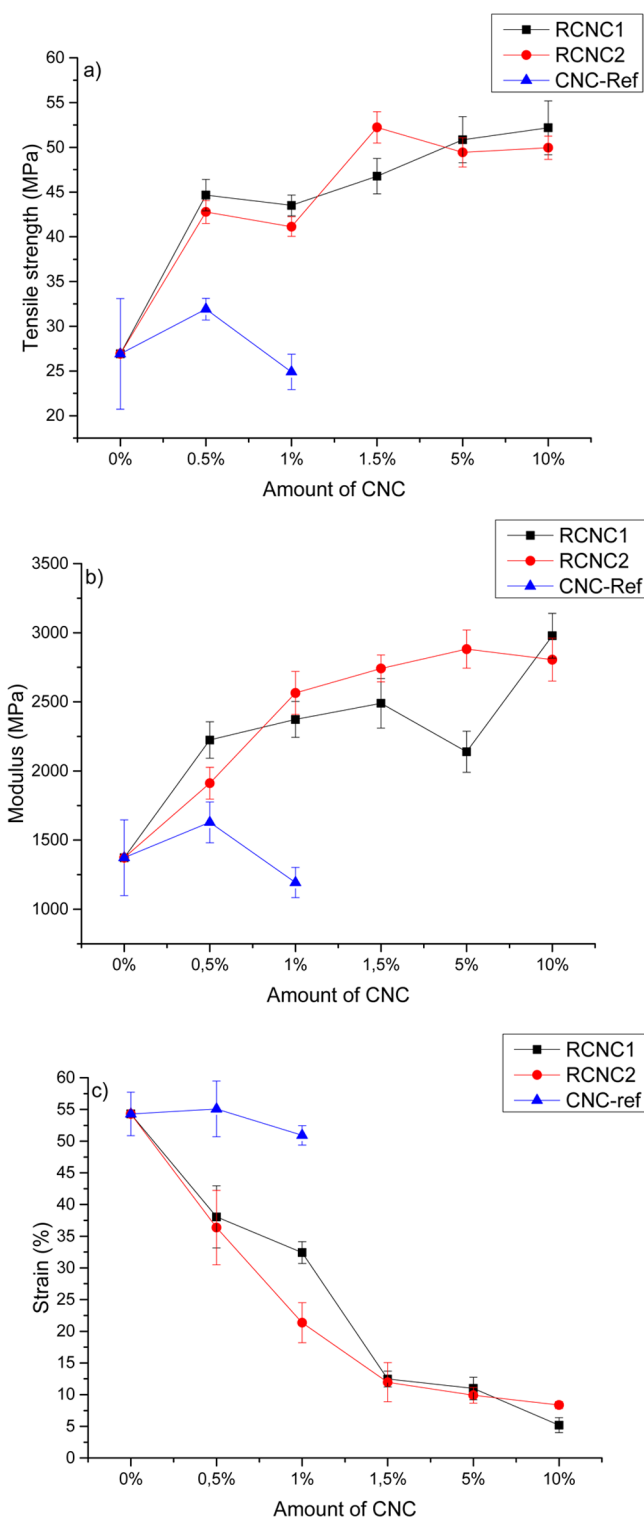
Figure 5. Mechanical properties of CNC-reinforced PVA films: (a) tensile strength, (b) modulus, and (c) strain (error bars represents standard error).

Figure 6. (a) OP and (b) WVP values of PVA, RCNCs-reinforced PVA films, and CNC-ref-reinforced PVA films (error bars represent standard error).

form stable, cyclic acetal bonds between the aldehydes of RCNCs, which is why this study used bifunctional RCNCs as potential reactive reinforcing agents for PVA films. Scheme 2 presents the cross-linking reaction of PVA with the aldehydes of RCNCs. An acetal cross-linking formation was not possible with CNC-ref, for which aldehydes were reduced to hydroxyl groups. Thus, CNC-ref was used to produce a reference film.
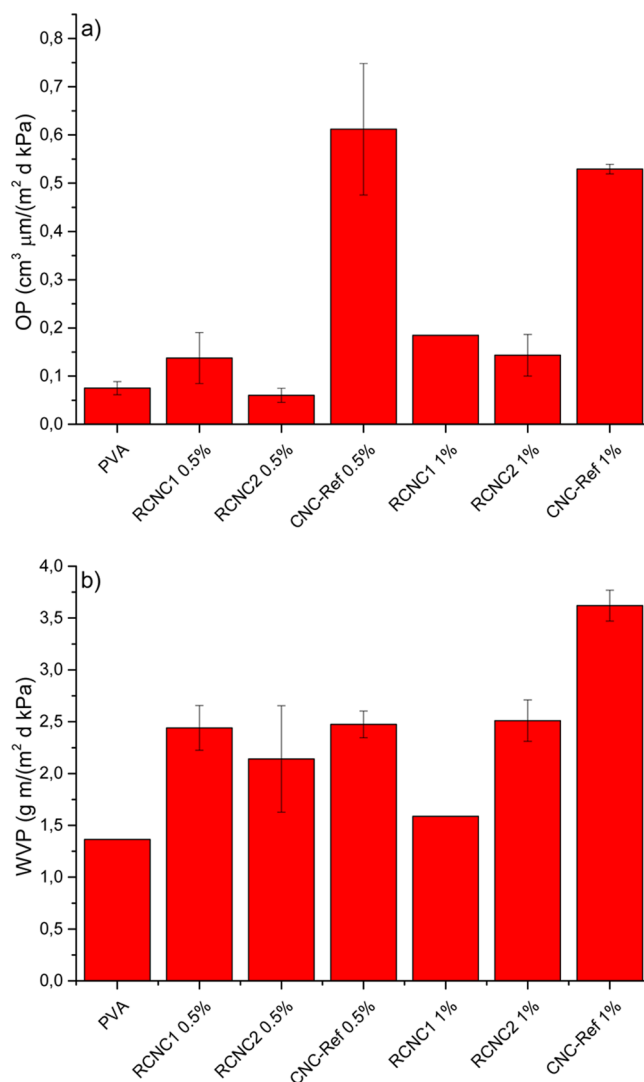
All CNCs resulted in highly transparent films for the studied CNC dosages (0.5−10 wt %) (Figure 4). The films were easy to handle at 50% RH, whereas all of the films, including the pure PVA film, became brittle at a normal humidity. Therefore, all of the film handling was done at 50% RH. Brittleness was most likely due to not using a plasticizer in order to better discern the role of CNCs in PVA reinforcement.

The addition of 0.5% RCNCs increased the tensile strength of PVA by 59−65%, depending on the RCNCs used (Figure 5). The reinforcing effect of RCNC1 increased relatively linearly, and the tensile strength of 52 MPa was obtained using 10% RCNC1, which is a 94% higher value compared to pure PVA film. When using RCNC2, the highest tensile strength (52 MPa) was found at 1.5%. Despite the differing aldehyde content, there were only minor differences between the reinforcing effects of the two RCNCs.

CNC-ref with reduced aldehyde groups exhibited a markedly lower effect of tensile strength than RCNCs in PVA film. For example, the tensile strength of PVA film with 0.5% CNC-ref was 13 MPa lower than film with 0.5% RCNC1. No significant difference was observed when comparing pure PVA film and
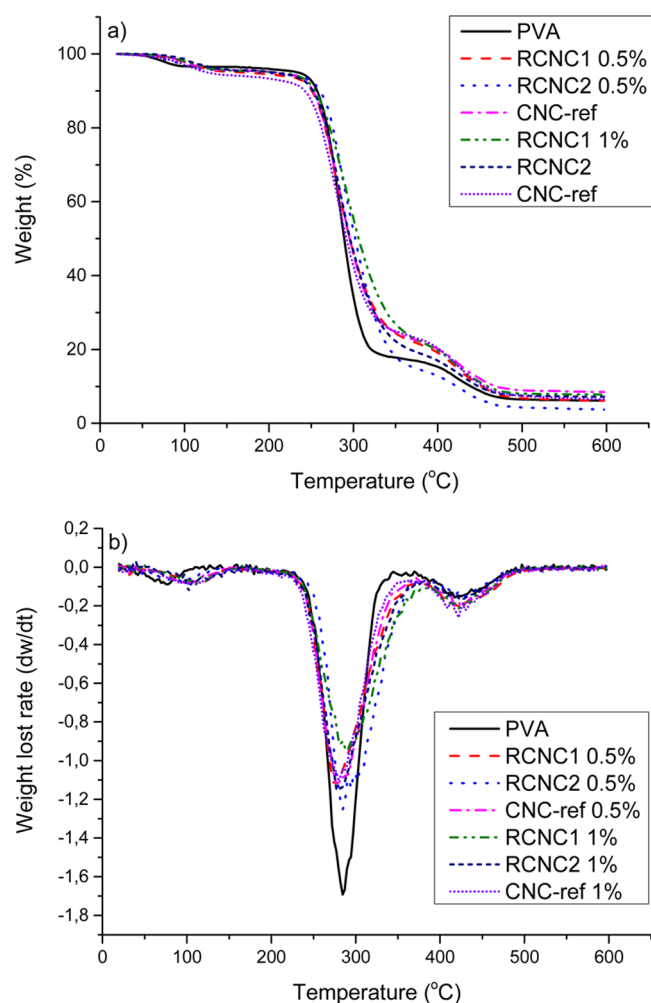
Figure 7. (a) TGA and (b) DTG curves of PVA, RCNCs-reinforced PVA films, and CNC-ref-reinforced PVA films.

film with 0.5% CNC-ref, and a decrease in strength was obtained when 1.0% CNC-ref was used.

The changes in Young's modulus were observed to be similar to the tensile strength effects. The use of 0.5% RCNC1 or RCNC2 resulted in an increase in the modulus of 59% and 39%, respectively. The highest modulus (2.9 GPa) was obtained using 5% RCNC2, which is 101% higher than pure PVA film. CNC-ref did not provide any improvement in the modulus of the PVA films. Strain of PVA-CNC films decreased gradually by the increase in the amount of RCNC1 and RCNC2 and no significant difference between samples could be observed. Strain of the PVA film decreased from 21% to 5% and 4% with 5% addition of RCNC1 and RCNC2, respectively. After further addition of RCNCs, there was only minor decrease in strain values. On the other hand, the addition of CNC-ref had no effect on the strain values which is consist with the strength and modulus values of PVA-CNC-ref films. The results of the mechanical properties of the PVA-CNC films indicate that the reinforcing effect of RCNCs on PVA film can likely be attributed to cross-linking via acetal bonds between the aldehyde functionalities of the CNCs and the hydroxyl groups of PVA.

Different reinforcing effects of CNCs on PVA films have previously been reported in the literature. Chen et al. and Fortunati et al. attained a 33% and 46% increase in the Young's modulus using CNCs obtained from potato peel waste[40] and okra fibers,[41] respectively. The use of CNCs consisting of 1% okra fiber was observed to decrease the modulus, which is similar to our results with CNC-ref. Pereira et al. reported an increase of up to 3% in the tensile strength using 3% CNCs isolated from banana pseudostems.[42] CNCs isolated from corncobs with a CNC loading of 3%, 6%, and 9% increased the tensile strength of PVA by 49.5%, 95.6%, and 140.2%, respectively.[43] The use of poly(acrylic acid) as a cross-linking agent resulted in a 150% increase in the tensile strength of PVA film with 10% CNCs,[27] although a relatively high amount of poly(acrylic acid) was required (10%).
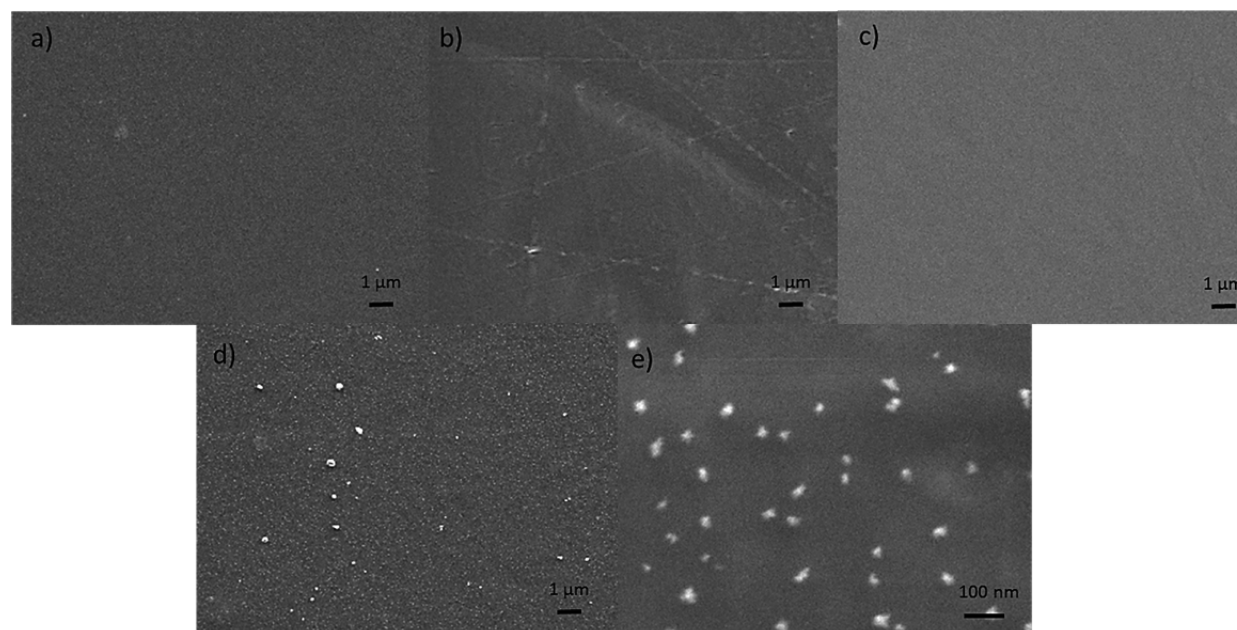

Figure 8. FESEM images of (a) pure PVA film, reinforcement films with 10% (b) RCNC1 and (c) RCNC2, and (d and e) 1% of CNC-ref. (Lines in panel (b) are due to the scratches on the surface of the film.)
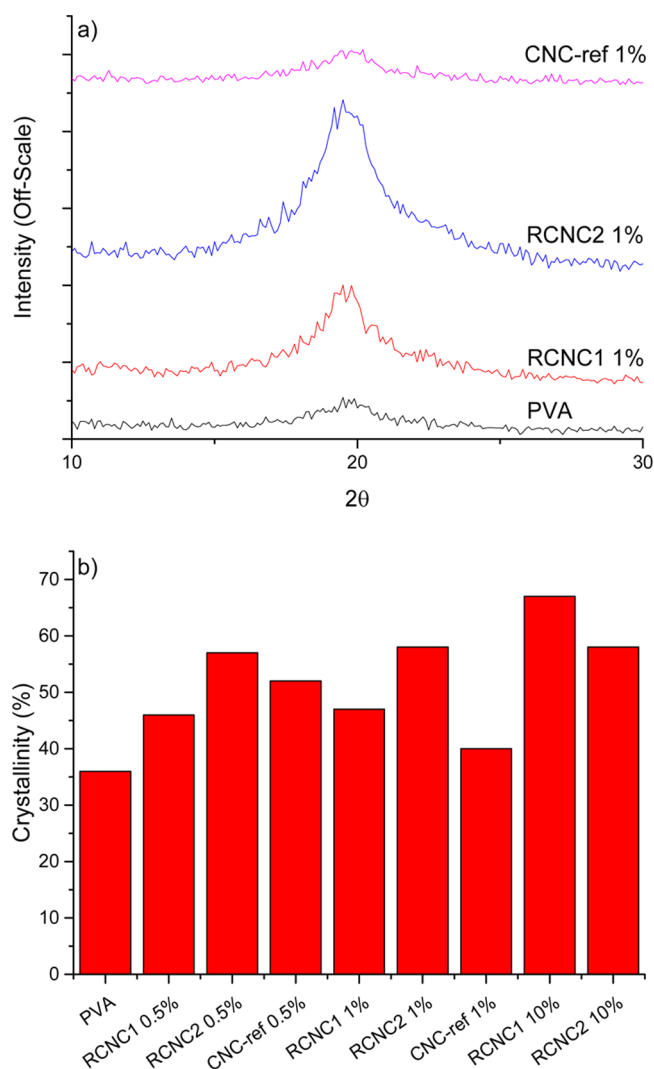
Figure 9. (a) Examples of WAXD diffractograms and (b) CrIs of PVA films.

The barrier properties of CNC-reinforced PVA films against oxygen and water vapor was studied using films with 0.5% and 1% CNC loading. The OP of pure PVA films increased from 0.075 cm³ μm/(m² d kPa) to 0.14 and 0.18 cm³ μm/(m² d kPa) with RCNC1 when 0.5% and 1% loading were used, respectively, indicating a decrease in the oxygen barrier resistance (Figure 6a). In contrast, when RCNC2 was used, a small decrease in OP was observed from 0.075 to 0.06 cm³ μm/ (m² d kPa) with a 0.5% addition. This finding suggests that a higher aldehyde group content may be beneficial for oxygen barrier properties. However, the RCNC 2 dosage of 1% resulted in a similar OP value as that obtained with RCNC1. 8-fold higher OP values were obtained by using CNC-ref as a reinforcing agent for PVA films, demonstrating the important role of cross-linking on barrier performance.

PVA is known for its high oxygen barrier performance, and although nanocellulose also generally maintains a good barrier against oxygen,[44] the addition of CNCs to PVA can be assumed to have a negative effect on barrier properties according to the mixing rule. For example, films of butylaminated CNCs produced from periodate-oxidized cellulose have previously been reported to have an order of magnitude higher OP value at 50% RH than that of PVA film.[45] Therefore, on the basis of

our results, it can be assumed that aldehyde functionalities and the formation of acetal bonds between PVA and RCNCs help prevent the decrease in PVA's oxygen barrier properties because no increase, or only a small increase in OP, was observed when RCNCs were added to PVA films.

The water vapor barrier of PVA films was observed to decrease when CNCs were added (Figure 6b). No significant difference in the WVP values was observed when RCNC1, RCNC2, or CNC-ref were used, except for CNC-ref at a dosage of 1%. The hydrophilic nature of cellulose, and especially its carboxylic acid functionalities, is the main reason for the increased WVP values of PVA films. An increase in the WVP was previously reported for PVA film reinforced with epoxy-NFC.[29]

All of the films showed an initial loss of weight at around 100 °C, which is associated with the evaporation of adsorbed water (Figure 7a). The onset temperature of the second thermal event for pure PVA film was 262 °C. This lost weight is due to the degradation of the PVA molecule and can be described as a first degradation event of PVA.[27] The onset temperature of the first degradation event for PVA-nanocellulose films was in the range of 254−265 °C, indicating similar thermal properties as pure PVA film. The onset temperature of the second degradation event for all of the samples was close to 400 °C. The first derivate curves of the TGA (DTG) curves show that the addition of nanocellulose significantly changes the rate of lost weight in the first degradation event (Figure 7b). For example, film containing 1% of RCNC1 had about a two times lower weight lost rate than that of pure PVA film. Similar behavior was found for other PVA-CNC composites.[23,41,46] These results indicate that the thermal properties of PVA are not degenerated by the addition of CNCs; however, the presence of CNCs can slow down the degradation of PVA.

Dispersion of RCNCs and CNC-ref to PVA was studied using SEM. According to Figure 8, the surfaces of PVA films containing RCNC1 and RCNC2 were smooth and similar to pure PVA films. Only few bigger, nonfibrillated fibers can be seen on the surface of the film containing 10% of RCNC1. The CNC-ref film had a high amount of small aggregates on the surface of the film with diameters around 300 to 20 nm. As the aggregates are absent in the surface of PVA and RCNCs reinforced films, it can be concluded that CNC-ref disperse poorly to PVA matrix, which may explain the inferior reinforcement effect of CNC-ref compared to RCNCs

Examples of WAXD diffractograms of PVA films are presented in Figure 9a. All of the films exhibited the characteristic crystalline maxima of PVA around 19.4°.[47] CrI of pure PVA film was increased from 36% to 40−67% by the addition of nanocelluloses (Figure 9b). The addition of nanosized fillers can enhance the nucleation of polymer,[48] which then increases the CrI.[49] No significant difference was observed between CNCs, except the relatively low CrI of the film containing 1% of CNC-ref, which might explain the poor mechanical properties of the film. Even though film containing 0.5% of CNC-ref had similar CrI than the films with RCNCs, aggregates observed in FESEM images might act as discontinuity points, which decrease the mechanical strength.

■ **CONCLUSIONS**

Periodate oxidation and partial chlorite oxidation were found to be efficient ways of obtaining bifunctional CNCs with reactive aldehyde functionalities. The use of this method allows the elimination of the difficult and cumbersome purification steps

because the chemical modifications can be performed prior to disintegration into CNCs. In addition, the entire reaction can be performed using water as a solvent. The produced RCNCs were found to be efficient reinforcing agents for PVA films. A notable increase in the tensile strength and in Young's modulus was achieved with the addition of only 0.5% RCNCs to PVA film. Aldehyde groups were found to be crucial in the reinforcement of PVA films: the use of reference CNCs without reactive aldehydes led to a significantly lower tensile strength and modulus. In addition, RCNCs retained the beneficial oxygen barrier properties of pure PVA.

■ AUTHOR INFORMATION

Corresponding Author
*Tel: +358294482424. Fax: +358 855 323 27. E-mail: Juho. Sirvio@oulu.fi.

Author Contributions
The manuscript was written through contributions of all authors. All authors have given approval to the final version of the manuscript.

Notes
The authors declare no competing financial interest.

■ ACKNOWLEDGMENTS

■ REFERENCES

(1) Henriksson, M.; Berglund, L. A.; Isaksson, P.; Lindström, T.; Nishino, T. Cellulose Nanopaper Structures of High Toughness. *Biomacromolecules* **2008**, *9* (6), 1579−1585.

(2) Kettunen, M.; Silvennoinen, R. J.; Houbenov, N.; Nykänen, A.; Ruokolainen, J.; Sainio, J.; Pore, V.; Kemell, M.; Ankerfors, M.; Lindström, T.; Ritala, M.; Ras, R. H. A.; Ikkala, O. Photoswitchable Superabsorbency Based on Nanocellulose Aerogels. *Adv. Funct. Mater.* **2011**, *21* (3), 510−517.

(3) Salas, C.; Nypelö, T.; Rodriguez-Abreu, C.; Carrillo, C.; Rojas, O. J. Nanocellulose Properties and Applications in Colloids and Interfaces. *Curr. Opin. Colloid Interface Sci.* **2014**, *19* (5), 383−396.

(4) Alexandrescu, L.; Syverud, K.; Gatti, A.; Chinga-Carrasco, G. Cytotoxicity Tests of Cellulose Nanofibril-Based Structures. *Cellulose* **2013**, *20* (4), 1765−1775.

(5) Pitkänen, M.; Kangas, H.; Laitinen, O.; Sneck, A.; Lahtinen, P.; Peresin, M. S.; Niinimäki, J. Characteristics and Safety of Nano-Sized Cellulose Fibrils. *Cellulose* **2014**, *21* (6), 3871−3886.

(6) Abdul Khalil, H. P. S.; Davoudpour, Y.; Islam, M. N.; Mustapha, A.; Sudesh, K.; Dungani, R.; Jawaid, M. Production and Modification of Nanofibrillated Cellulose Using Various Mechanical Processes: A Review. *Carbohydr. Polym.* **2014**, *99*, 649−665.

(7) Habibi, Y.; Lucia, L. A.; Rojas, O. J. Cellulose Nanocrystals: Chemistry, Self-Assembly, and Applications. *Chem. Rev.* **2010**, *110* (6), 3479−3500.

(8) Qin, Z.-Y.; Tong, G.-L.; Chin, Y. C. F.; Zhou, J.-C. Preparation of Ultrasonic-Assisted High Carboxylate Content Cellulose Nanocrystals by Tempo Oxidation. *BioResources* **2011**, *6* (2), 1136−1146.

(9) Leung, A. C. W.; Hrapovic, S.; Lam, E.; Liu, Y.; Male, K. B.; Mahmoud, K. A.; Luong, J. H. T. Characteristics and Properties of Carboxylated Cellulose Nanocrystals Prepared from a Novel One-Step Procedure. *Small* **2011**, *7* (3), 302−305.

(10) Visanko, M.; Liimatainen, H.; Sirviö, J. A.; Heiskanen, J. P.; Niinimäki, J.; Hormi, O. Amphiphilic Cellulose Nanocrystals from Acid-Free Oxidative Treatment: Physicochemical Characteristics and Use as an Oil−Water Stabilizer. *Biomacromolecules* **2014**, *15* (7), 2769−2775.

(11) Aranguren, M. I.; Marcovich, N. E.; Salgueiro, W.; Somoza, A. Effect of the Nano-Cellulose Content on the Properties of Reinforced Polyurethanes. A Study Using Mechanical Tests and Positron Anihilation Spectroscopy. *Polym. Test.* **2013**, *32* (1), 115−122.

(12) Pu, Y.; Zhang, J.; Elder, T.; Deng, Y.; Gatenholm, P.; Ragauskas, A. J. Investigation into Nanocellulosics Versus Acacia Reinforced Acrylic Films. *Composites, Part B* **2007**, *38* (3), 360−366.

(13) Lu, J.; Askeland, P.; Drzal, L. T. Surface Modification of Microfibrillated Cellulose for Epoxy Composite Applications. *Polymer* **2008**, *49* (5), 1285−1296.

(14) Sirviö, J. A.; Kolehmainen, A.; Liimatainen, H.; Niinimäki, J.; Hormi, O. E. O. Biocomposite Cellulose-Alginate Films: Promising Packaging Materials. *Food Chem.* **2014**, *151*, 343−351.

(15) Azeredo, H. M. C.; Mattoso, L. H. C.; Avena-Bustillos, R. J.; Filho, G. C.; Munford, M. L.; Wood, D.; McHugh, T. H. Nanocellulose Reinforced Chitosan Composite Films as Affected by Nanofiller Loading and Plasticizer Content. *J. Food Sci.* **2010**, *75* (1), N1−N7.

(16) Teixeira, E. de M.; Pasquini, D.; Curvelo, A. A. S.; Corradini, E.; Belgacem, M. N.; Dufresne, A. Cassava Bagasse Cellulose Nanofibrils Reinforced Thermoplastic Cassava Starch. *Carbohydr. Polym.* **2009**, *78* (3), 422−431.

(17) Flieger, M.; Kantorová, M.; Prell, A.; Řezanka, T.; Votruba, J. Biodegradable Plastics from Renewable Sources. *Folia Microbiol. (Dordrecht, Neth.)* **2003**, *48* (1), 27−44.

(18) Shang, Y.; Peng, Y. Research of a PVA Composite Ultrafiltration Membrane Used in Oil-in-Water. *Desalination* **2007**, *204* (1−3), 322−327.

(19) Alexy, P.; Káchová, D.; Kršiak, M.; Bakoš, D.; Šimková, B. Poly(vinyl alcohol) Stabilisation in Thermoplastic Processing. *Polym. Degrad. Stab.* **2002**, *78* (3), 413−421.

(20) Schmedlen, R. H.; Masters, K. S.; West, J. L. Photocrosslinkable Polyvinyl Alcohol Hydrogels That Can be Modified with Cell Adhesion Peptides for Use in Tissue Engineering. *Biomaterials* **2002**, *23* (22), 4325−4332.

(21) Gaume, J.; Wong-Wah-Chung, P.; Rivaton, A.; Thérias, S.; Gardette, J.-L. Photochemical Behavior of PVA as an Oxygen-Barrier Polymer for Solar Cell Encapsulation. *RSC Adv.* **2011**, *1* (8), 1471−1481.

(22) Kvien, I.; Oksman, K. Orientation of Cellulose Nanowhiskers in Polyvinyl Alcohol. *Appl. Phys. A: Mater. Sci. Process.* **2007**, *87* (4), 641−643.

(23) Qua, E. H.; Hornsby, P. R.; Sharma, H. S. S.; Lyons, G.; McCall, R. D. Preparation and Characterization of Poly(vinyl alcohol) Nanocomposites Made from Cellulose Nanofibers. *J. Appl. Polym. Sci.* **2009**, *113* (4), 2238−2247.

(24) Jalal Uddin, A.; Araki, J.; Gotoh, Y. Toward "Strong" Green Nanocomposites: Polyvinyl Alcohol Reinforced with Extremely Oriented Cellulose Whiskers. *Biomacromolecules* **2011**, *12* (3), 617−624.

(25) Peresin, M. S.; Habibi, Y.; Zoppe, J. O.; Pawlak, J. J.; Rojas, O. J. Nanofiber Composites of Polyvinyl Alcohol and Cellulose Nanocrystals: Manufacture and Characterization. *Biomacromolecules* **2010**, *11* (3), 674−681.

(26) Abitbol, T.; Johnstone, T.; Quinn, T. M.; Gray, D. G. Reinforcement with Cellulose Nanocrystals of Poly(vinyl alcohol) Hydrogels Prepared by Cyclic Freezing and Thawing. *Soft Matter* **2011**, *7* (6), 2373−2379.

(27) Paralikar, S. A.; Simonsen, J.; Lombardi, J. Poly(vinyl alcohol)/ Cellulose Nanocrystal Barrier Membranes. *J. Membr. Sci.* **2008**, *320* (1−2), 248−258.

(28) Song, Z.; Xiao, H.; Zhao, Y. Hydrophobic-Modified Nano-Cellulose Fiber/PLA Biodegradable Composites for Lowering Water

Vapor Transmission Rate (WVTR) of Paper. *Carbohydr. Polym.* **2014**, *111*, 442−448.

(29) Virtanen, S.; Vartianen, J.; Setälä, H.; Tammelin, T.; Vuoti, S. Modified Nanofibrillated Cellulose−Polyvinyl Alcohol Films with Improved Mechanical Performance. *RSC Adv.* **2014**, *4* (22), 11343−11350.

(30) Lin, N.; Bruzzese, C.; Dufresne, A. TEMPO-Oxidized Nanocellulose Participating as Crosslinking Aid for Alginate-Based Sponges. *ACS Appl. Mater. Interfaces* **2012**, *4* (9), 4948−4959.

(31) Liimatainen, H.; Sirviö, J.; Haapala, A.; Hormi, O.; Niinimäki, J. Characterization of Highly Accessible Cellulose Microfibers Generated by Wet Stirred Media Milling. *Carbohydr. Polym.* **2011**, *83* (4), 2005−2010.

(32) Sirvio, J.; Hyvakko, U.; Liimatainen, H.; Niinimaki, J.; Hormi, O. Periodate Oxidation of Cellulose at Elevated Temperatures Using Metal Salts as Cellulose Activators. *Carbohydr. Polym.* **2011**, *83* (3), 1293−1297.

(33) Sirviö, J. A.; Liimatainen, H.; Visanko, M.; Niinimäki, J. Optimization of Dicarboxylic Acid Cellulose Synthesis: Reaction Stoichiometry and Role of Hypochlorite Scavengers. *Carbohydr. Polym.* **2014**, *114*, 73.

(34) Katz, S.; Beatson, P. R.; Scallan, A. M. The Determination of Strong and Weak Acidic Groups in Sulfite Pulps. *Sven. Papperstidn.* **1984**, *87* (6), 48−53.

(35) Rattaz, A.; Mishra, S. P.; Chabot, B.; Daneault, C. Cellulose Nanofibres by Sonocatalysed-TEMPO-Oxidation. *Cellulose* **2011**, *18* (3), 585−593.

(36) Larsson, P. A.; Berglund, L. A.; Wågberg, L. Highly Ductile Fibres and Sheets by Core-Shell Structuring of the Cellulose Nanofibrils. *Cellulose* **2014**, *21* (1), 323−333.

(37) Gaidukov, S.; Danilenko, I.; Gaidukova, G. Characterization of Strong and Crystalline Polyvinyl Alcohol/Montmorillonite Films Prepared by Layer-by-Layer Deposition Method. *Int. J. Polym. Sci.* **2015**, *2015*, e123469.

(38) Rabiej, S.; Wlochowicz, A. SAXS and WAXS Investigations of the Crystallinity in Polymers. *Angew. Makromol. Chem.* **1990**, *175* (1), 81−97.

(39) Sirviö, J. A.; Hasa, T.; Ahola, J.; Liimatainen, H.; Niinimäki, J.; Hormi, O. Phosphonated Nanocelluloses from Sequential Oxidative-Reductive Treatment − Physicochemical Characteristics and Thermal Properties. *Carbohydr. Polym.* **2015**, *133*, 524.

(40) Chen, D.; Lawton, D.; Thompson, M. R.; Liu, Q. Biocomposites Reinforced with Cellulose Nanocrystals Derived from Potato Peel Waste. *Carbohydr. Polym.* **2012**, *90* (1), 709−716.

(41) Fortunati, E.; Puglia, D.; Monti, M.; Santulli, C.; Maniruzzaman, M.; Kenny, J. M. Cellulose Nanocrystals Extracted from Okra Fibers in PVA Nanocomposites. *J. Appl. Polym. Sci.* **2013**, *128* (5), 3220−3230.

(42) Pereira, A. L. S.; do Nascimento, D. M.; Souza Filho, M. de sá M.; Morais, J. P. S.; Vasconcelos, N. F.; Feitosa, J. P. A.; Brígida, A. I. S.; Rosa, M. de F. Improvement of Polyvinyl Alcohol Properties by Adding Nanocrystalline Cellulose Isolated from Banana pseudostems. *Carbohydr. Polym.* **2014**, *112*, 165−172.

(43) Silvério, H. A.; Flauzino Neto, W. P.; Pasquini, D. Effect of Incorporating Cellulose Nanocrystals from Corncob on the Tensile, Thermal and Barrier Properties of Poly(Vinyl Alcohol) Nanocomposites. *J. Nanomater.* **2013**, *2013*, e289641.

(44) Sirviö, J. A.; Kolehmainen, A.; Visanko, M.; Liimatainen, H.; Niinimaki, J.; Hormi, O. E. O. Strong, Self-Standing Oxygen Barrier Films from Nanocelluses Modified with Regioselective Oxidative Treatments. *ACS Appl. Mater. Interfaces* **2014**, *6*, 14384.

(45) Visanko, M.; Liimatainen, H.; Sirviö, J. A.; Mikkonen, K. S.; Tenkanen, M.; Sliz, R.; Hormi, O.; Niinimäki, J. Butylamino-Functionalized Cellulose Nanocrystal Films: Barrier Properties and Mechanical Strength. *RSC Adv.* **2015**, *5* (20), 15140−15146.

(46) Li, W.; Yue, J.; Liu, S. Preparation of Nanocrystalline Cellulose via Ultrasound and its Reinforcement Capability for Poly(vinyl alcohol) Composites. *Ultrason. Sonochem.* **2012**, *19* (3), 479−485.

(47) Assender, H. E.; Windle, A. H. Crystallinity in Poly(vinyl alcohol). 1. An X-ray Diffraction Study of Atactic PVOH. *Polymer* **1998**, *39* (18), 4295−4302.

(48) Alexandre, B.; Langevin, D.; Médéric, P.; Aubry, T.; Couderc, H.; Nguyen, Q. T.; Saiter, A.; Marais, S. Water Barrier Properties of Polyamide 12/Montmorillonite Nanocomposite Membranes: Structure and Volume Fraction Effects. *J. Membr. Sci.* **2009**, *328* (1−2), 186−204.

(49) Lani, N. S.; Ngadi, N.; Johari, A.; Jusoh, M. Isolation, Characterization, and Application of Nanocellulose from Oil Palm Empty Fruit Bunch Fiber as Nanocomposites. *J. Nanomater.* **2014**, *2014*, e702538.